

ON THE ENERGY DISTRIBUTION OF SPUTTERED DIMERS

G. P. KÖNNEN, A. TIP and A. E. DE VRIES

*FOM-Instituut voor Atoom- en Molecuulfysica, Kruislaan 407,
Amsterdam/Wgm., The Netherlands*

(Received September 27, 1973)

A theoretical expression is obtained for the energy distribution of sputtered dimers from crystal surfaces. The derivation is based on a model where the atoms which constitute a dimer, are sputtered independently from the crystal according to their respective single particle energy distribution functions. Two neighbouring atoms are then supposed to form a dimer if the sum of their initial relative kinetic energy and potential energy is less than zero. A comparison with experimental results for K_2 and KI sputtered from polycrystalline K and KI surfaces respectively, shows a good agreement.

1 INTRODUCTION

Although it is known for several years that sputtering results in the ejection of both monatomic and polyatomic particles, only in the last few years the energy distributions of some charged¹⁻⁴ and neutral⁵⁻⁷ sputtered clusters have been reported.

A few attempts have been undertaken to explain the observed energy distributions of the sputtered clusters, which appear to be hyperthermal and show a more rapid fall-off to zero than the monomer distributions. Joyes⁸ calculated the mean energy of sputtered Cu_2 dimers, assuming that the dimer receives its energy from another Cu atom from the target. Baede, Jungmann and Los⁶ compared the energy distribution of K_2 dimers sputtered from polycrystalline K with a thermal spike theory. Staudenmaier² proposed a model in which the clusters are assumed to be formed from the individual atoms leaving the collisions cascade, and in which the different binding energies of the various clusters with respect to the surfaces determine their ejection probabilities. In this paper we present a dimer sputtering model which assumes that all dimers are formed from recombination of two simultaneously sputtered atoms. Assuming the initial energy distribution of these atoms to be independent of each other, we calculated the dimer energy distributions from the monomer distributions. A comparison of the experimental data with this independent particle model shows that the model explains the observed energy distribution of the dimers very well.

2 THE MECHANISM OF DIMER FORMATION

In this section a precise formulation of the adopted mechanism for dimer formation is given. The basic assumptions are the following:

1) Particles belonging to a single collision cascade leave the surface at the same time t_0 .

2) The constituent particles of a dimer belong to the same collision cascade. Two such particles form a dimer if at the initial time t_0 the sum of their potential energy $V(r_0)$ and their relative kinetic energy ϵ does not exceed zero:

$$V(r_0) + \epsilon \leq 0 \quad (2.1)$$

3) The formation of trimers and higher polymers is excluded.

In order to perform numerical calculations some further assumptions will be made:

4) All particles belonging to a collision cascade are sputtered independently, their initial distribution function $\phi(E, \Omega)$ (E is the kinetic energy, Ω the solid angle) being given by the corresponding monomer distribution function.

5) The monomer energy distribution function f_j of species j is given by

$$f_j(E, \Omega) = N_j E(E + E_b^{(j)})^{-(n_j+1)} \cos \lambda \quad (2.2)$$

where $E_b^{(j)}$ is the binding energy of an atom of species j with the surface, n_j is a constant, N_j a

normalization constant and λ is the angle with the normal to the surface. Formula (2.2) is obtained from the assumption that in the collision cascade the energy distribution of atom j is proportional to E^{-n_j} .^{9,10}

In many cases condition (2.1) excludes the formation of dimers from particles which are initially not neighbours. This is due to the circumstance that usually $V(r_0)$ is close to zero for such a pair of particles, whereas ϵ is always positive. If, on the other hand, the two particles are neighbours, then it makes sense to approximate $V(r_0)$ by $-E_d$ where E_d is the dissociation energy of the dimer. Thus:

6) Dimers are formed only from neighbouring atoms in the lattice. Their formation is subject to the condition

$$\epsilon \leq E_d \quad (2.3)$$

The above assumptions allow the calculation of the energy and angle dependence of the dimer distribution function. For the normal direction the velocity distribution of the dimers dS/dv is found to be (see section 3):

$$\begin{aligned} \frac{dS}{dv} &= 2\pi N_1 N_2 (m_1 + m_2) \\ &\cdot \int_0^{(2\mu E_d)^{1/2}} d\xi \cdot \xi^2 \int_{-\min(1, m_1 v/\xi)}^{\min(1, m_2 v/\xi)} dz (m_1 v + \xi z)(m_2 v - \xi z) \\ &\cdot [m_1 v^2 + \xi^2 + 2m_1 v \xi z + 2m_1 E_b^{(1)}]^{-(n_1+1)} \\ &\cdot [m_2 v^2 + \xi^2 - 2m_2 v \xi z + 2m_2 E_b^{(2)}]^{-(n_2+1)} \quad (2.4) \end{aligned}$$

in which m_1 and m_2 are the masses of particles 1 and 2, μ their reduced mass, and N_1 and N_2 the normalization constants of the monomer distributions. From this one obtains the energy distribution dS/dE through the relation

$$\frac{dS}{dE} = \frac{dS}{dv} \cdot \frac{dv}{dE} \propto v^{-1} \frac{dS}{dv} \quad (2.5)$$

dS/dE behaves as follows: it starts linearly from zero, passes through a maximum and falls off to zero at high energies as $E^{-n_1-n_2-1.5}$, which is indeed much more rapidly than the energy distributions of the monomers.

The behaviour of this function is illustrated in Figure 1 on a log-log plot for a homonuclear dimer X_2 with $E_d = 0.5$ eV, $E_b = 1.0$ eV and $n = 1.5$. It is not possible to obtain a better than order of magnitude estimate for the ratio of monomers and dimers at a given energy and in a given direction. For this a

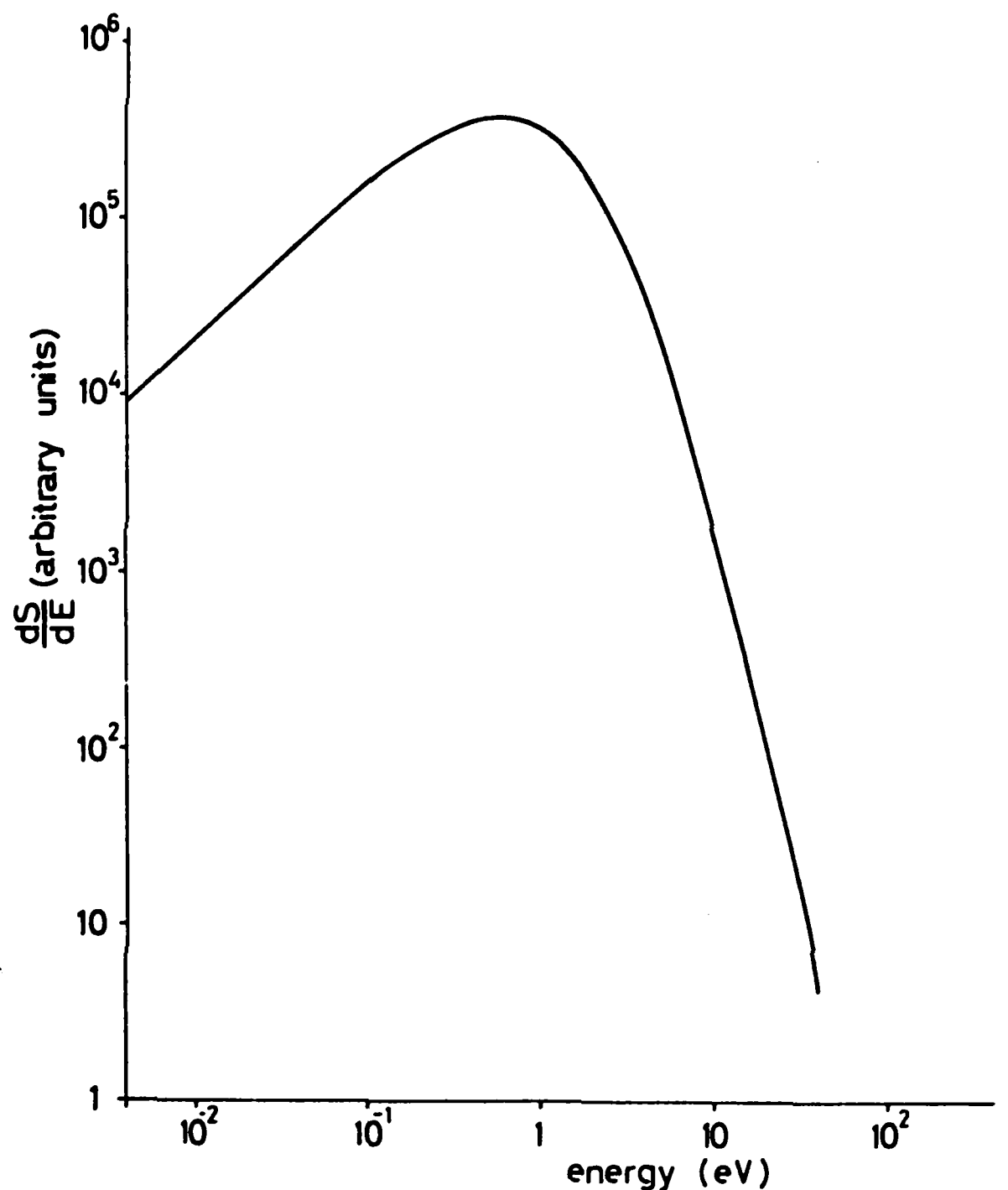


FIGURE 1 The energy distribution of dimers X_2 , calculated from the atomic energy distribution with $E_d = 0.5$ eV, $E_b = 1$ eV and $n = 1.5$.

specific knowledge is needed about the statistics of the occurrence of the various configurations at the surface of particles to be sputtered.

3 THE CALCULATION OF THE DIMER DISTRIBUTION FUNCTION

3.1 The Distribution Function

According to the model put forward in the previous section, the calculation of the dimer distribution function amounts to a calculation of the available phase-space under condition (2.3). The normalized probability density for two neighbouring particles to have relative energy ϵ and centre-of-mass velocity \mathbf{V} is given by

$$w(\epsilon, \mathbf{V}) = \int d\mathbf{p}_1 \int d\mathbf{p}_2 \phi_1(\mathbf{p}_1) \phi_2(\mathbf{p}_2) \delta(\epsilon - E_{\text{rel}}) \delta(\mathbf{V} - \mathbf{V}_{\text{cm}}) \quad (3.1)$$

Here \mathbf{p} is the momentum vector of particle j and $\phi_j(\mathbf{p}_j)$ is the normalized momentum distribution function for sputtered monomers of species j . The relative

energy E_{rel} and centre-of-mass velocity \mathbf{V}_{cm} are given by

$$E_{\text{rel}} = \frac{1}{2}\mu(\mathbf{p}_1/m_1 - \mathbf{p}_2/m_2)^2, \quad \mathbf{V}_{\text{cm}} = M^{-1}(\mathbf{p}_1 + \mathbf{p}_2) \quad (3.2)$$

where m_j is the mass of a particle of species j , $M = m_1 + m_2$ and $\mu = m_1 m_2 / M$.

After a change to centre-of-mass and relative variables according to

$$\mathbf{P} = \mathbf{p}_1 + \mathbf{p}_2, \quad \mathbf{p} = \mu(\mathbf{p}_1/m_1 - \mathbf{p}_2/m_2), \quad (3.3)$$

$w(\epsilon, \mathbf{V})$ can be written as

$$w(\epsilon, \mathbf{V}) = \int d\mathbf{P} \int d\mathbf{p} \phi_1((m_1/M)\mathbf{P} + \mathbf{p}) \phi_2((m_2/M)\mathbf{P} - \mathbf{p}) \cdot \delta(\epsilon - p^2/2\mu) \delta(\mathbf{V} - \mathbf{P}/M) = 2M\mu \int d\mathbf{p} \phi_1(m_1\mathbf{V} + \mathbf{p}) \cdot \phi_2(m_2\mathbf{V} - \mathbf{p}) \cdot \delta(p^2 - 2\mu\epsilon)$$

The remaining δ -function can be removed by means of the identity

$$\delta(p^2 - 2\mu\epsilon) = \frac{1}{2}(2\mu\epsilon)^{-1/2} \{ \delta(p - (2\mu\epsilon)^{1/2}) + \delta(p + (2\mu\epsilon)^{1/2}) \} \quad (3.4)$$

To achieve this \mathbf{p} is written as $\mathbf{p} = pu$, u being the unit vector along \mathbf{p} . Then $d\mathbf{p} = p^2 dp du$, du indicating an integration over a solid angle, and

$$w(\epsilon, \mathbf{V}) = 2M\mu \int_0^\infty dp \cdot p^2 \int du \phi_1(m_1\mathbf{V} + pu) \cdot \phi_2(m_2\mathbf{V} - pu) \cdot \frac{1}{2}\zeta^{-1} \{ \delta(p - \zeta) + \delta(p + \zeta) \} = M\mu\zeta \int du \phi_1(m_1\mathbf{V} + \zeta\mathbf{u}) \phi_2(m_2\mathbf{V} - \zeta\mathbf{u}) \quad (3.5)$$

with

$$\zeta = (2\mu\epsilon)^{1/2} \quad (3.6)$$

From this the normalized dimer distribution function $w(\mathbf{V})$ is obtained by integration over ϵ from zero to E_d ;

$$w(\mathbf{V}) = \int_0^{E_d} d\epsilon w(\epsilon, \mathbf{V}) = M \int_0^{(2\mu E_d)^{1/2}} d\zeta \cdot \zeta^2 \int du \cdot \phi_1(m_1\mathbf{V} + \zeta\mathbf{u}) \cdot \phi_2(m_2\mathbf{V} - \zeta\mathbf{u}) \quad (3.7)$$

Thus $w(\mathbf{V})$ is the normalized probability density for finding a dimer with velocity \mathbf{V} , i.e. with an energy $E = V^2/(2M)$ in the direction of \mathbf{V} . In order to proceed it is necessary to substitute explicit expressions for the $\phi_j(\mathbf{p}_j)$. The relation between $\phi(\mathbf{p})$ and $f(E, \Omega)$ given by (2.2) is (the subscript j is dropped for the moment):

$$f(E, \Omega) dE d\Omega = K \phi(\mathbf{p}) d\mathbf{p}, \quad E = p^2/(2m), \quad d\mathbf{p} = p^2 dp d\Omega \quad (3.8)$$

where K is a proportionality constant. From this the

following normalized monomer momentum distribution is obtained for species j :

$$\phi_j(\mathbf{p}_j) = N_j (\mathbf{p}_j \cdot \mathbf{e}) h((\mathbf{p}_j \cdot \mathbf{e})) \cdot (p_j^2 + L_j)^{-(n_j+1)} \quad (3.9)$$

Here \mathbf{e} is the unit vector normal to the surface,

$$N_j = 2n_j(n_j - 1)L_j^{n_j-1}/\pi, \quad L_j = 2m_j E_b^{(j)} \quad (3.10)$$

and the Heaviside step function $h((\mathbf{p}_j \cdot \mathbf{e}))$ ($h(x) = 0$, $x < 0$ and $h(x) = 1$, $x \geq 0$) takes into account that sputtering only takes place in one half space. Since $w(\mathbf{V})$ is symmetric about \mathbf{e} , \mathbf{V} can be fixed in the YZ -plane in a coordinate system with \mathbf{e} along the positive Z -axis. The angle between \mathbf{V} and \mathbf{e} will be denoted by θ . Let the polar angles of \mathbf{u} be ϑ and ψ , so that

$$\mathbf{V} \cdot \mathbf{e} = V \cos \theta \quad \mathbf{V} \cdot \mathbf{u} = V(\sin \theta \sin \vartheta \sin \psi + \cos \theta \cos \vartheta) \\ \mathbf{u} \cdot \mathbf{e} = \cos \vartheta \quad d\mathbf{u} = \sin \vartheta d\vartheta d\psi \quad (3.11)$$

Then

$$w(\mathbf{V}) = w(V, \theta) = MN_1 N_2 \int_0^{(2\mu E_d)^{1/2}} d\zeta \cdot \zeta^2 \int_0^{2\pi} d\psi \cdot \int_0^\pi d\vartheta \cdot \sin \vartheta \cdot \\ \cdot (m_1 V \cos \theta + \zeta \cos \vartheta) h(m_1 V \cos \theta + \zeta \cos \vartheta) \\ \cdot (m_2 V \cos \theta - \zeta \cos \vartheta) h(m_2 V \cos \theta - \zeta \cos \vartheta) \\ \cdot [m_1^2 V^2 + \zeta^2 + 2m_1 V \zeta (\sin \vartheta \sin \vartheta \sin \psi + \cos \theta \cos \vartheta) + L_1]^{-(n_1+1)} \\ \cdot [m_2^2 V^2 + \zeta^2 - 2m_2 V \zeta (\sin \theta \sin \vartheta \sin \psi + \cos \theta \cos \vartheta) + L_2]^{-(n_2+1)}.$$

It is convenient to change from ϑ to $z = \cos \vartheta$. Then the Heaviside functions can be replaced by a condition on the integration interval for z :

$$w(V, \theta) = MN_1 N_2 \int_0^{(2\mu E_d)^{1/2}} d\zeta \cdot \zeta^2 \int_0^{2\pi} d\psi \int_{-\min(1, m_1 V \cos \theta / \zeta)}^{+\min(1, m_2 V \cos \theta / \zeta)} dz \\ \cdot (m_1 V \cos \theta + \zeta z) (m_2 V \cos \theta - \zeta z) \\ \cdot [m_1^2 V^2 + \zeta^2 + 2m_1 V \zeta \{ \sin \theta (1 - z^2)^{1/2} \cdot \sin \psi + z \cos \theta \} + L_1]^{-(n_1+1)} \\ \cdot [m_2^2 V^2 + \zeta^2 - 2m_2 V \zeta \{ \sin \theta (1 - z^2)^{1/2} \cdot \sin \psi + z \cos \theta \} + L_2]^{-(n_2+1)} \quad (3.12)$$

This is the final expression for the distribution function of sputtered dimers. For the case $\theta = 0$, i.e. sputtering of dimers in the direction normal to the surface it

simplifies significantly:

$$w(V, 0) =$$

$$2\pi MN_1 N_2 \int_0^{(2\mu E_d)^{1/2}} d\xi \cdot \xi^2 \cdot \int_{-\min(1, m_1 V/\xi)}^{+\min(1, m_2 V/\xi)} dz \cdot (m_1 V + \xi z)(m_2 V - \xi z) \cdot [m_1^2 V^2 + \xi^2 + 2m_1 V \xi z + L_1]^{-(n_1+1)} \cdot [m_2^2 V^2 + \xi^2 - 2m_2 V \xi z + L_2]^{-(n_2+1)} \quad (3.13)$$

In Section 4 the results of numerical calculations of this expression are given and compared with experimental data on dimer sputtering.

3.2 Asymptotic Behaviour

It is not difficult to obtain from (3.12) the behaviour of $w(V, \theta)$ for V tending to infinity and zero, respectively. In the first case it is even more convenient to turn to the expression (3.7) for $w(V)$. For large absolute values of V the term ξu in the argument of ϕ_j can be neglected, since ξ ranges through the bounded interval $[0, (2\mu E_d)^{1/2}]$. Thus, for V tending to infinity:

$$w(V, \theta) \sim M \int_0^{(2\mu E_d)^{1/2}} d\xi \cdot \xi^2 \cdot \int du \phi_1(m_1 V) \phi_2(m_2 V) \sim (4\pi/3) \cdot MN_1 N_2 \cdot m_1^{-(2n_1+1)} m_2^{-(2n_2+1)} \cdot (2\mu E_d)^{3/2} \cdot V^{-2(n_1+n_2+1)} \cos^2 \theta \quad (3.14)$$

The behaviour of $w(V, \theta)$ for V tending to zero is obtained in the following way. It is convenient to split $w(V, \theta)$ into four parts and to consider each part separately. Thus for $\theta < \pi/2$:

$$w(V, \theta) = \int_0^{m_2 V \cos \theta} d\xi \int_0^1 dz \dots + \int_0^{(2\mu E_d)^{1/2}} d\xi \int_0^{m_2 V \cos \theta/\xi} dz \dots + \int_0^{m_1 V \cos \theta} d\xi \int_{-1}^0 dz \dots + \int_{-m_1 V \cos \theta/\xi}^0 dz \dots = \sum_{j=1}^4 w_j(V, \theta) \quad (3.15)$$

For small V the terms L_1 and L_2 in the denominator become the leading terms in $w_1(V, \theta)$ so that

$$w_1(V, \theta) \sim 2\pi MN_1 N_2 L_1^{-(n_1+1)} L_2^{-(n_2+1)} \cdot \int_0^{m_2 V \cos \theta} d\xi \cdot \xi^2 \cdot \int_0^1 dz (m_1 V \cos \theta + \xi z) \cdot (m_2 V \cos \theta - \xi z) = 2\pi MN_1 N_2 [(5/24)m_1 m_2^4 + (7/120)m_2^5] \cdot L_1^{-(n_1+1)} L_2^{-(n_2+1)} (V \cos \theta)^5 \quad (3.16)$$

By interchanging the subscripts 1 and 2 the corresponding expression for $w_3(V, \theta)$ is obtained. In $w_2(V, \theta)$ and $w_4(V, \theta)$ the leading term in the denominator is $[\xi^2 + L_1]^{-(n_1+1)} [\xi^2 + L_2]^{-(n_2+1)}$ since now ξ ranges up to $(2\mu E_d)^{1/2}$, instead of $m_j V \cos \theta$, $j = 1, 2$ in the former case. Thus, for V tending to zero:

$$w_2(V, \theta) \sim 2\pi MN_1 N_2 \int_0^{(2\mu E_d)^{1/2}} d\xi \cdot \xi^2 \cdot \int_0^{m_2 V \cos \theta/\xi} dz \cdot (m_1 V \cos \theta + \xi z)(m_2 V \cos \theta - \xi z) \cdot [\xi^2 + L_1]^{-(n_1+1)} [\xi^2 + L_2]^{-(n_2+1)} \sim 2\pi MN_1 N_2 (\frac{1}{2} m_1 m_2^2 + 1/6 m_2^3) \int_0^{(2\mu E_d)^{1/2}} d\xi \cdot \xi [\xi^2 + L_1]^{-(n_1+1)} [\xi^2 + L_2]^{-(n_2+1)} \cdot V^3 \cos^3 \theta, \quad (3.17)$$

and the corresponding expression for $w_4(V, \theta)$ is obtained by interchanging the subscripts 1 and 2. Comparing the result with (3.16) it is seen that $w_2(V, \theta)$ and $w_4(V, \theta)$ are the leading terms for V tending to zero. Hence, for V tending to zero:

$$w(V, \theta) \sim 2\pi MN_1 N_2 (\frac{1}{2} m_1 m_2^2 + \frac{1}{2} m_1^2 m_2 + (1/6) m_1^3 + (1/6) m_2^3) \cdot \int_0^{(2\mu E_d)^{1/2}} d\xi \cdot \xi [\xi^2 + L_1]^{-(n_1+1)} \cdot [\xi^2 + L_2]^{-(n_2+1)} V^3 \cos^3 \theta \quad (3.18)$$

4 COMPARISON WITH EXPERIMENTS

To compare the present theory with experimental data, one has to know the parameters E_b and n of the energy distribution of the monomers. However, only for the systems K_2 and KI enough experimental data on the monomer distributions are available to make this comparison possible. In this section we will discuss these two cases.

4.1 The K_2 Distribution

Baede, Jungmann and Los⁶ measured the energy distribution of K_2 dimers sputtered from a polycrystalline K target under Ar^+ ion bombardment of 8, 11 and 13 keV kinetic energy. The sputtered K and K_2 neutrals were separated by an inhomogeneous magnet and measured by a surface ionisation detector. The energy distribution of the dimers was found to be independent of the Ar^+ energy. The measured signals were corrected for scattering on the background gas. There were indications that part of the signal was due to reflected atoms. Assuming the number of dimers to be zero at 4 eV kinetic energy, the measured points were also corrected for this effect. However, since evidence was obtained from chemi ionization experiments that alkali dimers are still present at 5 eV kinetic energy, this last correction was considered to be too crude. The true K_2 spectrum was supposed to lie between the corrected and uncorrected points.

In the experimental set up of Baede *et al.* the particles were detected under an angle of 22.5° with respect to the normal of the target. However, the large Ar^+ current causes damage of the target surface after a short time so that the direction of the normal of the target becomes quite undefined. For the theoretical energy distribution we therefore used formula (2.4) and (2.5) for the normal direction.

In Figure 2 the experimental points of Baede *et al.* are compared with the present theory. Since Baede

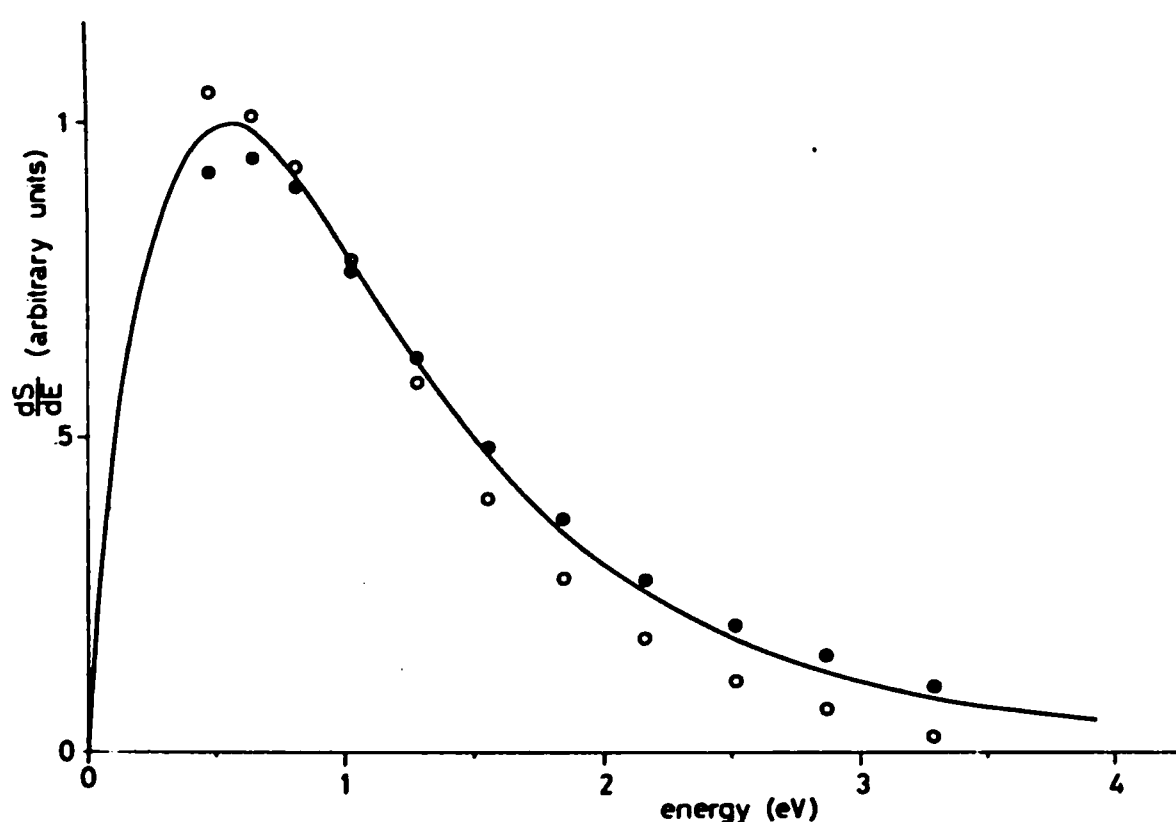


FIGURE 2 The energy distribution of K_2 dimers sputtered from a polycrystalline K target. The solid line represents the theoretical curve with $E_d = 0.55$ eV, $E_b = 0.71$ eV and $n = 1.525$. The open and closed circles are the measured points by Baede *et al.*, respectively with and without the two corrections discussed in the text. The theoretical curve and experimental points have been normalized at 1.1 eV.

reported the quantity $E \cdot (dS/dE)$ as a function of energy, his measured points have been divided by a factor E to obtain the energy distribution dS/dE . The parameters of the monomer distribution are taken from measurements of Politiek and Kistemaker,¹⁰ giving $n = 1.525$ and $E_b = 0.71$ eV for K sputtered from polycrystalline K under 8 keV Ar^+ bombardment. E_d was chosen to be 0.55 eV, which is the dissociation energy of K_2 molecules in the gasphase.¹¹ The open and closed circles in the figure are the measured points of Baede *et al.*, with and without the two corrections discussed above. The measured points and the theoretical curve have been normalized at 1.1 eV, as is the case in Baede's plot.

The theoretical curve coincides well with the experimental points, lying indeed between the open and closed circles as is expected to be the case for the true experimental K_2 energy distribution. It seems that the present theory explains the experimental data better than the thermal spike model does, which was applied by Baede, also since the latter model leads to an improbably high spike temperature of 7820 K.

4.2 The KI Energy Distribution

The energy distributions of K, I, KI and K_2I_2 sputtered from a polycrystalline KI target under 6 keV Ar^+ ion bombardment were obtained recently.⁷

The I, KI and K_2I_2 distributions were measured by mass spectroscopy, while for the K distribution positive surface ionization was used. The parameter n was found to be 2 for I atoms and 1.5 for K atoms.

The parameter E_b is more difficult to obtain from the monomer distributions since one can expect that formation of polymers will lower the original atom distributions. However, the velocity and direction of a heavy I atom will not change very much if a K atom sticks to it. So, if one adds the measured I, KI and twice the K_2I_2 fluxes as a function of velocity for a given direction, the sum thus obtained represents to a good approximation the initial I velocity distribution. From the distribution found in this way we got $E_b = 0.4$ eV. This rather low value of E_b agrees with the measured one for the halogens from NaF and KCl, being respectively 0.26 and 0.31 eV.¹² For K atoms E_b was inferred from the observed similarity of the K atom distribution from polycrystalline KCl, KBr, KI and K targets, which indicates that the binding energy of a K atom on the alkali halides must be the same as for the alkali metal, giving $E_b = 0.7$ eV.

A theoretical calculation indeed yields $E_b = 0.7$ eV for K from KCl^{13} and in view of the foregoing remark we therefore adopted this value also for KI.

Finally the dissociation energy E_d of KI is known to be 3.3 eV.¹¹ In this experiment the detectors were placed in the direction of the normal of the target and the energy distribution of the dimers was again calculated from formula (2.4) and (2.5). In Figure 3 the experimental curve is compared with the theory.

The uncertainty of the measured points for KI increases with decreasing energy. The best values were obtained for energies above 4 eV by suppressing the

background signal. The curves have been normalized by fitting the experimental points at an energy of 4.2 eV.

Finally dividing the dimer- by the monomer-intensity at a given energy by means of Eqs. (2.2), (2.4) and (2.5) the absolute height of this ratio was calculated. As explained in Section 2 this value can be expected to indicate only the order of magnitude of the real dimer to monomer ratio. Nevertheless the calculated ratios were found to agree with the experimental ones within a factor two for both K_2 and KI.

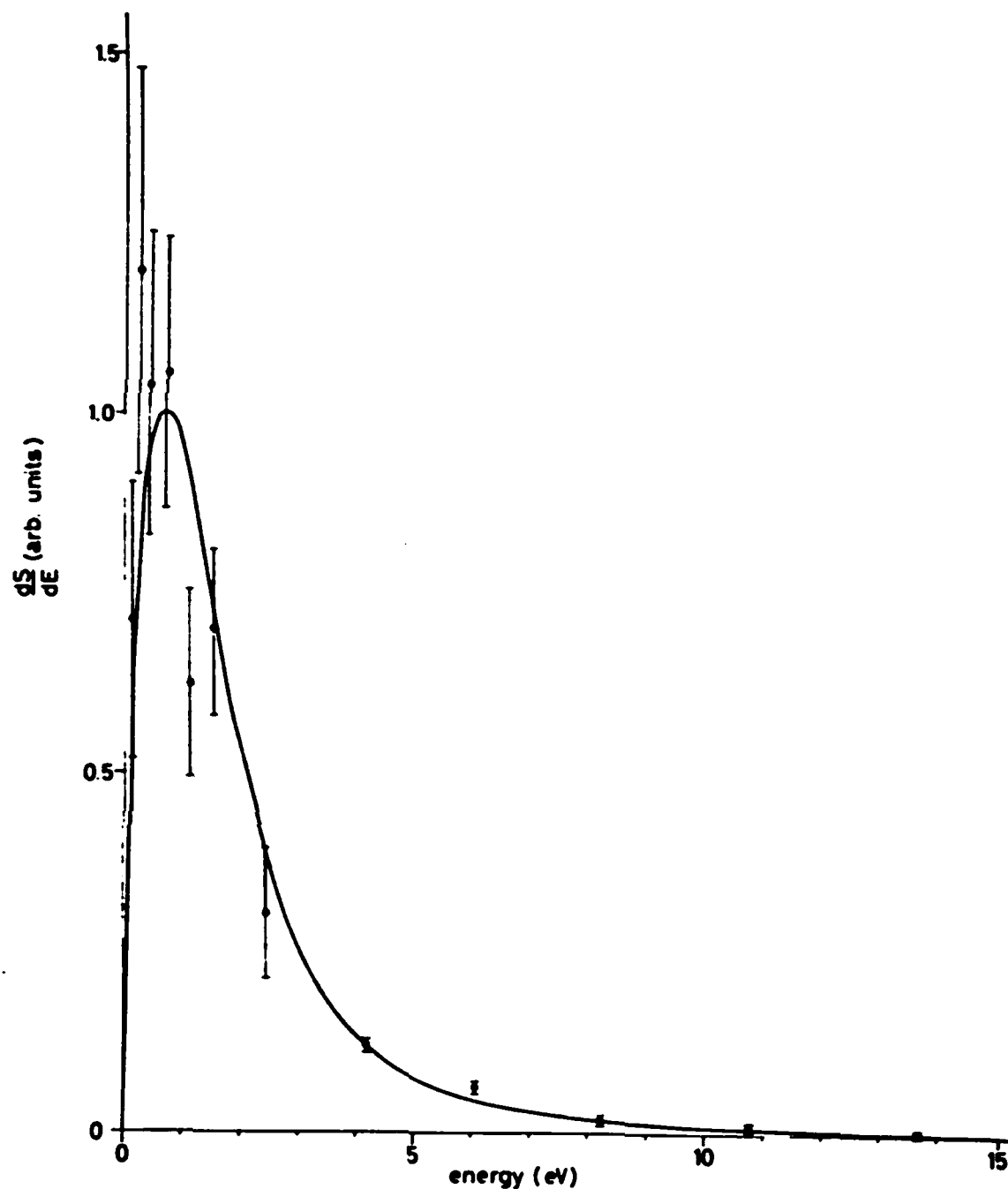


FIGURE 3 The energy distribution of KI. The solid line represents the theoretical curve with $n = 2$ and $E_b = 0.4$ eV for I, $n = 1.5$ and $E_b = 0.7$ eV for K; $E_d = 3.3$ eV. The closed points are the experimental data. The curve has been normalized at 4.2 eV.

ACKNOWLEDGEMENTS

This work is part of the research program of the Stichting voor Fundamenteel Onderzoek der Materie (Foundation of Fundamental Research on Matter) and was made possible by financial support of the Nederlandse Organisatie voor Zuiver-Wetenschappelijk Onderzoek (Netherlands Organization for the Advancement of Pure Research).

REFERENCES

1. Z. Jurela and B. Perović, *Can. J. Phys.* **46**, 773 (1968).
2. G. Staudenmaier, *Rad. Eff.* **13**, 87 (1972).
3. E. Dennis and R. J. MacDonald, *Rad. Eff.* **13**, 243. (1972).
4. R. K. F. Herzog, W. P. Poschenrieder and F. G. Satkiewicz, *Rad. Eff.* **18**, 199 (1973).
5. F. Schmidt-Bleek, G. Ostrom and S. Datz, *Rev. Sci. Instr.* **40**, 1351 (1969).
6. A. P. M. Baede, W. F. Jungmann and J. Los, *Physica* **54**, 459 (1971).
7. G. P. Können, J. Grosser, A. Haring, A. E. de Vries and J. Kistemaker, *Rad. Eff.* **21**, 171 (1974).
8. P. Joyes, *J. Phys. B* **4**, L 15 (1971).
9. M. W. Thompson, *Phil. Mag.* **18**, 377 (1968).
10. J. Politiek and J. Kistemaker, *Rad. Eff.* **2**, 129 (1969).
11. Handbook of Chemistry and Physics 1972-1973.
12. I. G. Higginbotham, T. E. Gallon, M. Pruton and H. Tokutaka, *Surface Sci.* **21**, 241 (1970).
13. J. E. Hove, *Phys. Rev.* **99**, 430 (1955).